



Contents lists available at ScienceDirect

Spectrochimica Acta Part A: Molecular and Biomolecular Spectroscopy

journal homepage: www.elsevier.com/locate/saa

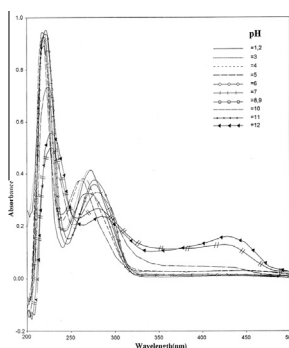
Spectroscopic studies on gallic acid and its azo derivatives and their iron(III) complexes

Mamdouh S. Masoud^a, Alaa E. Ali^{b,*}, Sawsan S. Haggag^a, Nessma M. Nasr^c^a Chemistry Department, Faculty of Science, Alexandria University, Alexandria, Egypt^b Chemistry Department, Faculty of Science, Damanhour University, Damanhour, Egypt^c Faculty of Pharmacy, Alexandria University, Alexandria, Egypt

HIGHLIGHTS

- The effect of pH on the absorption spectra of gallic acid and its azo derivatives is studied.
- The dissociation constants of the azo ligands are evaluated.
- Different spectroscopic methods are applied for determination of pK values of gallic acid–iron(III) complex.

GRAPHICAL ABSTRACT

Effect of pH on the electronic absorption spectra of 4×10^{-5} M of gallic acid.

ARTICLE INFO

Article history:

Received 7 May 2013

Received in revised form 8 October 2013

Accepted 10 October 2013

Available online 23 October 2013

Keywords:

Gallic acid

Dissociation constants

Spectrophotometric methods

Synthesis

Complexes

DTA

ABSTRACT

Azo gallic derivatives and their iron(III) complexes were synthesized and characterized. The stereochemistry and the mode of bonding of the complexes were achieved based on elemental analysis, UV–Vis and IR. The thermal behaviors of the complexes were studied. The effect of pH on the electronic absorption spectra of gallic acid and its azo derivatives are discussed. Different spectroscopic methods (molar ratio, straight line method, continuous variation, slope ratio and successive method) are applied for determination of stoichiometry and pK values for the complex formation of gallic acid with iron(III) in aqueous media. Iron(III) complexes of gallic acid is formed with different ratio: 1:1, 1:2, 1:3 and 1:4 (M:L).

© 2013 Elsevier B.V. All rights reserved.

Introduction

Gallic acid (3,4,5-trihydroxy benzoic acid) is a strong chelating agent and forms complexes of high stability with iron [1], where

the complexation starts from pH = 3 and continuous to pH = 9. The degree of chelation increases with increasing the pH. Iron is attached to gallic acid through two adjacent OH [2]. The kinetics and mechanisms of the reactions of a number of pyrogallol-based ligands with iron(III) have been investigated in aqueous solution at 25 °C and an ionic strength 0.5M NaClO₄, where 1:1 complex is formed initially, when the metal reacts with ligand subsequently

* Corresponding author. Tel.: +20 1115799866; fax: +20 4553293011.

E-mail address: dralaa@yahoo.com (A.E. Ali).

through an electron transfer reaction, with an evidence for the formation of 1:2 at higher pH-values [3]. When excess of iron(III) is added to an acidic solution of either gallic-acid or its methyl ester, a dark blue color appears initially and then rapidly fades, ascribed to the formation of 1:1 complex, in which the metal ion is coordinated to two adjacent hydroxyl groups of the ligand, while the third hydroxyl group remains protonated due to its high pK_a [4]. This is subsequently decomposed to Fe(II) and the corresponding semiquinone and then reacts rapidly with another Fe(III) species to form the quinone. Iron(III)–gallic acid complex shows, a maxima at 415 and 690 nm. The quinone absorbs at 380 nm with a shoulder at 445 nm. Gallic acid forms (1:3) complex with iron in the pH range 4–6 [5]. Kinetic study on the complexation of gallic acid with ferrous sulfate was performed using UV–Vis absorption spectroscopy. The stoichiometry composition of the formed complex is 1:1 [6] and the absorption band of gallic acid at 263 nm undergoes a bathochromic shift of 34 nm with the addition of ferrous ions, due to the formation of gallic acid–Fe(II) complex with the formation of a new absorption band at 570 nm, which is assigned to the complex formation. In the present manuscript, it is aimed to give more information about the chemistry of gallic acid and three azo compounds of groups of different electronic characters and some complexes especially Fe(III). The scope of the studies is itemized as follows: (i) studies on the free ligands (effect of pH on the electronic absorption spectra and evaluation of pK values), (ii) studies on the transition metal complexes (interaction of Fe(III) with gallic acid and evaluation of the possible species exist and their stabilities), (iii) synthesis and characterization of some solid complexes by elemental analysis, spectroscopy and magnetic moments) and thermal analysis (DTA) of some ligands and their complexes.

Experimental

The UV–VIS spectra were measured with a Perkin Elmer Lambda 4B spectrophotometer. Gallic acid and ferric chloride compounds were purchased from Sigma and Aldrich. 0.01 M stock solution of Fe(III) was prepared by dissolving the required weight in distilled water. The solution was acidified by the addition of hydrochloric acid to keep the Fe(III) soluble in water and the exact concentration was achieved complexometrically using salicylic acid as indicator. 0.01 M stock solution of gallic acid was prepared. For every new experiment fresh solution was prepared because gallic acid in aqueous solution does not persist for a long time. It oxidizes to quinone. Universal buffer solution was prepared by taking 0.04 M each of H_3BO_3 , H_3PO_4 and CH_3COOH acids and adding the required volume of 0.2 M NaOH to give the desired pH [7]. The pH was checked by using a Jenway 3015 pH-meter, previously calibrated with standard buffer solutions of pH 4.00, 7.02 and 9.18. 0.10 M KCl solutions were prepared and used to adjust the ionic strength of the solutions. 30 mmol of the ligand was dissolved in alcohol mixed with 15 m-mole of iron(III) chloride, which was dissolved in water. The reaction mixture was refluxed for one hour, and then left over-night, where the precipitated complexes were separated by filtration and washed by H_2O and dried in a desiccator over anhydrous $CaCl_2$. Azo compounds were prepared in a similar way by the usual diazotization process [8]. The required substituted amines (0.1 mol) were dissolved in (0.2 mol) HCl and 25 ml distilled water. The hydrochloride compounds were diazotized below 5 °C with a solution of $NaNO_2$ (0.1 mol) and 20 ml distilled water. The diazonium chloride was coupled with an alkaline solution of gallic acid (0.1 mol/30 ml distilled water). The crude dyes were filtered off and crystallized, then dried in a vacuum desiccator over P_4O_{10} . Fig. 1 illustrated the structures of gallic acid and its azo derivatives.

Results and discussion

Studies on the free ligands

Effect of pH on the electronic absorption spectra of gallic acid

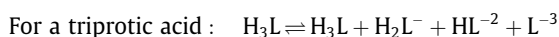
Fig. 2 is taken as a representative example for the effect of pH on the electronic absorption spectra of 4×10^{-5} solution of gallic acid, which showed three well defined bands with λ_{max} at 230, 280 and 425 nm. The first two bands are due to $\pi-\pi^*$ transition, while the last one is due to $n-\pi^*$ transition. The acidity constants of gallic acid are $pK_1 = 4.9$, $pK_2 = 7.5$, $pK_3 = 10.3$ [1]. The ionization mechanism of gallic acid proceeds in two steps. The first acidity constant is associated with ionization of carboxylic group (1B). The second one is likely to be associated with the OH group in the 4-positions (1C), because this allows the delocalization of the negative charge and the presence of two ortho-positioned OH groups. This stabilizes the negative charge by intramolecular hydrogen bonds (1E), which lies lower in energy than structure (1F). In acidic medium [9], below pH = 3.4, gallic acid exists in its neutral form with its absorbance maximum at 269 nm. By increasing the pH gradually, the anion form of gallic acid exists, which shifts the absorbance maximum to 257 nm. However, from pH 4.5 to 7.5, the shift of maximum is small. Further increase of pH > 7, leads to the formation of a new additional peak with a maximum at 295 nm. At basic pH, gallic acid undergoes fast autooxidation, which leads to colorization of the solution. The peak with a maximum at 225 nm at pH = 2 gradually shifts to 231 nm at pH = 7. However, H_4L^2 shows two bands at 225 and 380 nm. Meanwhile, H_5L^3 gave four bands at 225, 260, 350 and 450 nm. Finally, H_5L^4 compound gave three bands at 225, 280 and 450 nm with one isosbestic point at $\lambda_{max} = 346$ nm. Remarkable features are given, where the compounds H_4L^1 , H_4L^2 and H_5L^3 possess no isosbestic point, probably due to the overlapping of absorbing species. The shorter wavelength region is due to the electronic transitions (up to ~250 nm) mainly of the $\pi-\pi^*$ type, while the longer wavelength side (>225 nm) can be argued to the electronic transitions mainly of $n-\pi^*$ type. The introduction of azo group affects the mode of ionization to some extent. In general, the azo compounds undergo a regular bathochromic shift on increasing the pH as a result of proton elimination. The aryl azo substituents exert an acid strength effect on the ligands (as will be seen later from the pK values).

Evaluation of pK -values

Different spectrophotometric methods deduced from As-pH relations were applied, half height [10], modified limiting absorption [11] and collector methods [12]. The data are collected in Table 1. Most of compounds under investigation give slopes = 1, 2 indicating one and two protons are ionized. In case of gallic acid, the slope = 3 leads to be completely tautomerized.

Distribution diagrams for gallic acid and its azo derivatives at different pH

From the distribution diagram plots between the fractions of an acid species of the ligands plotted against pH, we can find that the variation of these species are due to the acid dissociation is shifting as pH changes [13].



For H_4L^1 compound only three ionizable protons are traced, if the pH is 2.0 or less where the acid exists in the form of H_3L . It seems that the H_2L^- predominates in the pH range 4.5–6.5. However, on increasing the pH from 8.0–10.0, the HL^{-2} species

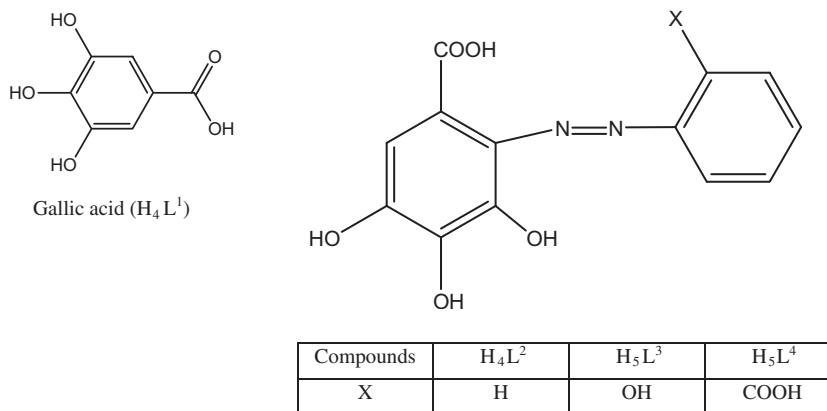


Fig. 1. Structures of gallic acid and its azo derivatives.

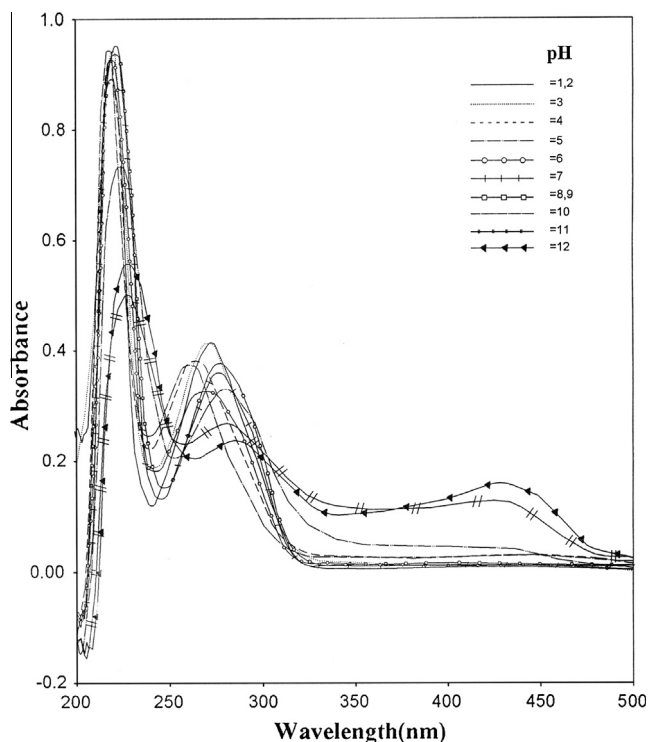


Fig. 2. Effect of pH on the electronic absorption spectra of 4×10^{-5} M of H₄L¹.

predominates, on further increasing the pH up to 12.0 or higher, the predominant species is L⁻³, while in case of H₄L², if the pH is less than 3.2, HL exists, on further increasing the pH up to 5.0 or higher, the L species exists. The compounds H₅L³ and H₅L⁴ are of

similar trend, where only two protons are traced. However, in case of H₅L³, for pH = 4.0, the compound exists in the form of H₂L, on increasing the pH from 6.5 to 8.0, so the predominant species is HL⁻, and if the pH > 10.5, the L⁻² exists. Meanwhile, in case of H₅L⁴, if the pH = 6.0, the predominant species is H₂L, on increasing the pH from 8.0 to 10.0, the predominant species is HL⁻ and if the pH is greater than 12.0, the compound exists in the form of L⁻². In case of H₅L³, the values of the slopes are 1.7 and 1.3. This suggests that the mechanism of -OH ionization is of complicated equilibria accompanied by the existence of an associated structure through intermolecular hydrogen bonding through two hydroxy groups and or intramolecular hydrogen bonding between the OH and N=N groups. However, in case of H₅L⁴, the values of the slopes are 1.5 and 0.6, which may support the presence of such intramolecular hydrogen bonding between the azo group and the O-COOH.

Studies on the Fe(III)-complexes

Interaction of Fe(III)-gallic acid and evaluation of the possible species exist and their stabilities

Molar-ratio method [14]. Fig. 3 represents the electronic absorption spectra of Fe(III)-gallic acid complex. The concentration of Fe(III) is kept constant at 4×10^{-4} M, while that of ligand is varied between 1×10^{-4} – 1.1×10^{-3} M. The stoichiometry of the reaction is obtained by plotting the absorbance of the resulting solution against the molar ratio of the variable concentration of the ligand with respect to that of Fe(III). It seems that the complex reaction by this procedure produced through 1:2 M ratios, Fig. 4.

Straight line method [15]. The following equation is applied:

$$\frac{1}{v^n} = \left(\frac{CD}{K_c} \cdot \frac{1}{A_s} \right) - \frac{D}{K_c} \quad (1)$$

By plotting $1/v_n$ against $1/A_s$, where ($n = 1, 2, 3$), a straight line is obtained at the proper stoichiometry of the reaction, Fig. 5. It is

Table 1
Dissociation constants of the organic compounds spectrophotometrically.

Compound	Half height			Modified limiting method			Collector			Average pK		
	pK ₁	pK ₂	pK ₃	pK ₁	pK ₂	pK ₃	pK ₁	pK ₂	pK ₃	pK ₁	pK ₂	pK ₃
H ₄ L ¹	4.9	7.5	10.3	4.3(2)	7.1(3.2)	9.6(0.8)	4.6	6.9	10.2	4.6 ± 0.3	7.1 ± 0.30	10.1 ± 0.37
H ₄ L ²	3.3	–	–	3.0(1.2)	–	–	3.3	–	–	3.2 ± 0.15	–	–
H ₅ L ³	4.2	9.2	–	4.9(1.7)	9.1(2.0)	–	4.4	9.3	–	4.5 ± 0.3	9.2 ± 0.1	–
H ₅ L ⁴	7.7	10.5	–	7.7(1.5)	10.1(0.6)	–	7.6	10.3	–	7.6 ± 0.05	10.2 ± 0.2	–

The value between brackets denotes the slope from the linear plots.

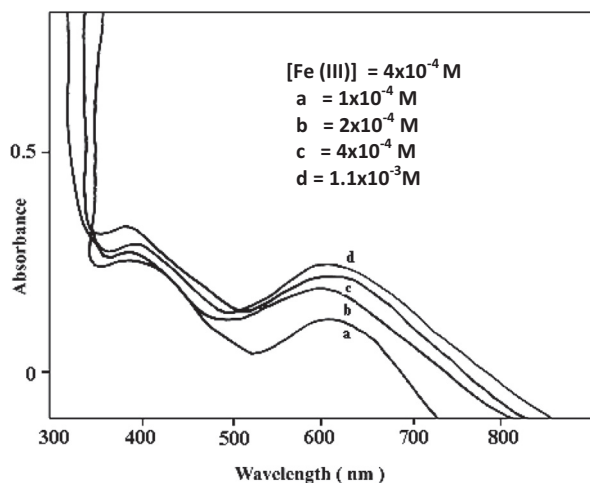


Fig. 3. Electronic absorption spectra of iron(III)-gallic acid in aqueous medium.

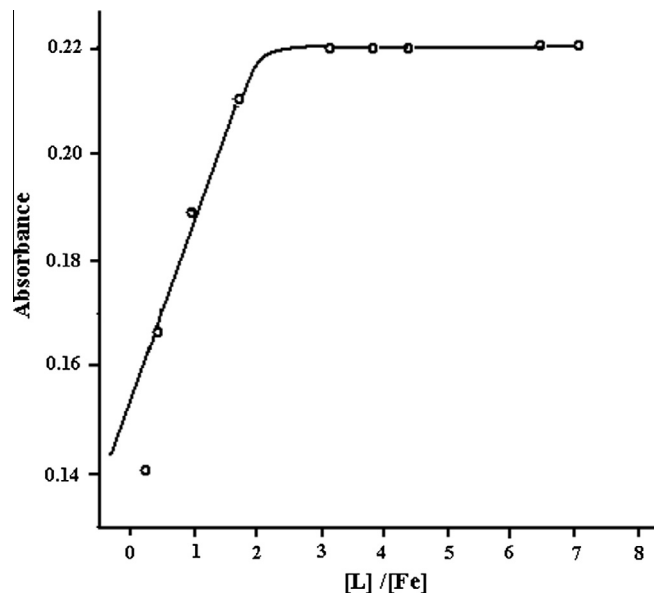


Fig. 4. Molar ratio plot for iron(III)-gallic acid reaction at $\lambda_{\max} = 600$ nm.

apparent that $n = 1$ is the predominant to assign the presence of a complex with a stoichiometry 1:1. If the complex is strongly dissociated:

$$\frac{K_c}{D} \cdot \frac{1}{v^n} \gg 1 \quad \therefore \log A_s = \log \frac{CD}{K_c} + n \log v \quad (2)$$

Plotting $\log A_s$ versus $\log v$, a straight line is obtained from which n and $\log(\frac{CD}{K_c})$ values are evaluated from the slope and the intercept, respectively. So, the stoichiometry and the equilibrium constants are calculated. The pK value is found to be 8.3.

The continuous variation method [16,17]. In this reaction, the total molar concentration is kept constant at 2×10^{-3} M. The measurement was done at $\lambda_{\max} = 386$ nm, Fig. 6. The extrapolation of such plot, gives 0.2, 0.35 and 0.45 mol fraction of Fe(III) to suggest the presence of complexes of 1:4, 1:2 and 1:1, respectively.

The slope ratio and the limiting logarithmic methods [14]. These methods are used to trace the complex formation in dilute

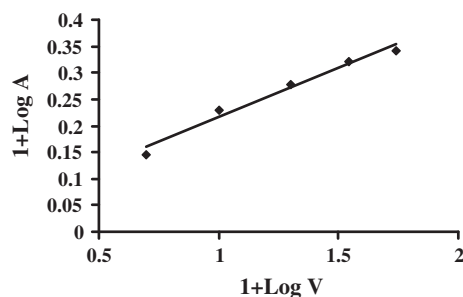


Fig. 5. Straight line logarithmic plot for iron(III)-gallic acid reaction at $\lambda_{\max} = 600$ nm.

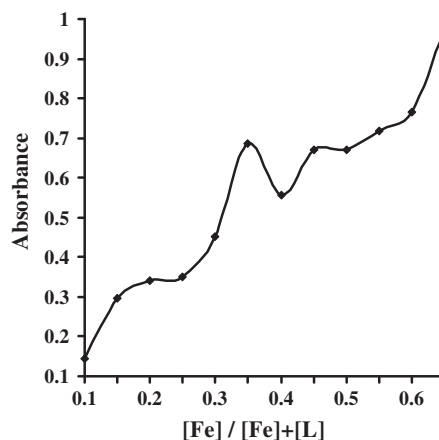


Fig. 6. Continuous variation method for iron(III)-gallic acid reaction at $\lambda_{\max} = 380$ nm.

solutions by taking two sets of experiments, Fig. 7. (i) The concentration of the ligand is kept constant in excess at (2×10^{-3} M), while that of iron(III) is varied between (1×10^{-4} – 6×10^{-4} M), (ii) the concentration of the iron(III) is kept constant in excess at (2×10^{-3} M), while that of the ligand is varied between (1×10^{-4} – 6×10^{-4} M). The absorbance of the two sets of solutions was measured at $\lambda_{\max} = 400$ nm. The limiting absorption method [18] is based on the same mode of thinking given before for the slope ratio method. On plotting the logarithmic values of the absorbance versus the logarithmic values of the concentration of the variable, Fig. 8. The stoichiometry of the complex reaction is calculated based on the ratio of the slopes of the two straight lines obtained. So, the traced complex is with the stoichiometry 1:1. It is observed from, Fig. 7b, in which, a straight line is obtained passed through the origin, indicating that the complexes formed obey Beer's law. The high ϵ value 762.4 is an advantage for applications, where very low concentrations in the pH-scale could be obtained.

The successive method [19]. This depends on the changing of both the concentration of the ligand and the metal ion. The following equation is applied, where A_s is the absorbance due to [ML], q is the molar extinction coefficient of the formed complex.

$$\therefore \frac{C_M C_{L^-}}{A_s} = \frac{1}{q\epsilon} + \frac{1}{\epsilon} (C_M + C_{L^-})$$

By plotting the left-hand side of the above equation versus $(C_M + C_{L^-})$, a straight line is obtained with a slope equals to $1/\epsilon$ and an intercept of $1/q\epsilon$. The results are diagrammed in Fig. 9. The values of molecular extinction (ϵ) and the formation constant (q)

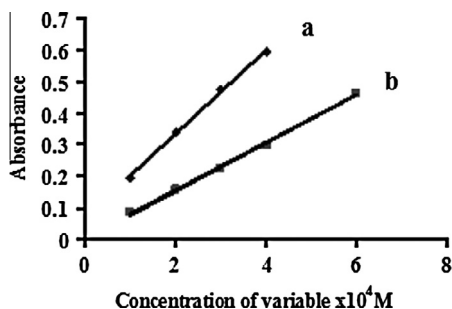


Fig. 7. Slope ratio method for iron(III)-gallic acid reaction at $\lambda_{\max} = 600$ nm. (a) $[\text{Fe}(\text{III})] = 2 \times 10^{-3}$, $[\text{L}]$ is variable, (b) $[\text{L}] = 2 \times 10^{-3}$, $[\text{Fe}(\text{III})]$ is variable.

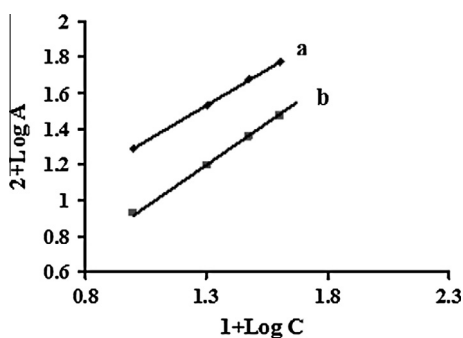


Fig. 8. Limiting logarithmic method for iron(III)-gallic acid reaction at $\lambda_{\max} = 400$ nm. (a) $[\text{Fe}^{3+}] = 2 \times 10^{-3}$, $[\text{L}]$ is variable, (b) $[\text{L}] = 2 \times 10^{-3}$, $[\text{Fe}(\text{III})]$ is variable.

are 11280 and 72900, respectively. The pK values obtained from different spectrophotometric methods are summarized in Table 2.

Synthesis and characterization of some solid complexes by elemental analysis, spectroscopy and magnetic moments

The infrared spectrum of the metal complexes, Table 3, compared with those of the frequencies of coordinated functional groups (e.g. ν_{OH} , $\nu_{\text{C=O}}$, $\nu_{\text{N=N}}$) are affected with different degrees depending on the strength of π -interaction occurring between the metal ion and π -electrons of the functional groups. Some of the carbonyl bands are disappeared, and others are slightly shifted, probably due to tautomerization to enol form followed by complexation through deprotonation. The IR of gallic acid gave three bands at 3494, 3279 and 2669 cm^{-1} , which are assigned to ν_{OH} . In case of $[\text{Fe}(\text{H}_4\text{L}^1)_3\text{Cl}_3 \cdot 4\text{H}_2\text{O}]$ complex, the three bands are shifted at 3410, 3341 and 2679 cm^{-1} , where phenolic OH groups are participating in the formation of the complexes [20]. However, in case of H_4L^2 and H_5L^4 , three bands are appeared at 3452, 3218, 3033 cm^{-1} and 3367, 3203, 3072 cm^{-1} , respectively, while H_5L^3 li-

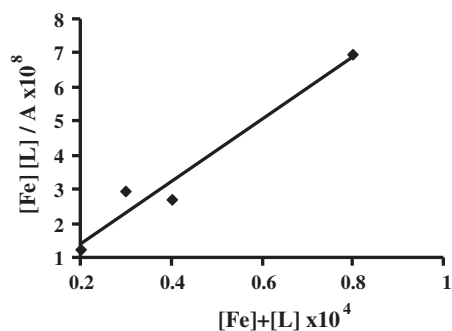
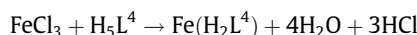
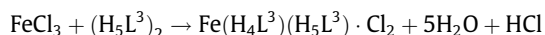
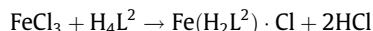
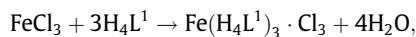


Fig. 9. Successive method for iron(III)-gallic acid reaction at $\lambda_{\max} = 271$ nm.

Table 2
pK values and the stoichiometry for iron(III)-gallic acid complex by using different spectroscopic methods.

Methods	Stoichiometry of iron(III)-gallic acid complexes	pK
Molar ratio	1:2	–
Straight line	1:1	8.30
Continuous variation	1:1	3.63
	1:2	6.43
	1:4	8.40
Slope ratio	1:1	–
Limiting logarithmic	1:1	–

gand gave a broad band at 3312 cm^{-1} assigned to ν_{OH} [21–23], where some changes occur on complexation. The data in such region are related either to that the $-\text{OH}$ group is affected on coordination or due to the existence of water molecule. Hydrogen bonded structures are expected due to intermolecular H-bonding between the azo group and the o-carboxy [24,25], H-bonding of the type $\text{O}-\text{H} \cdots \text{N}$ between the $-\text{OH}$ or $-\text{COOH}$ substituent and the $\text{N}=\text{N}$ group. The $\nu_{\text{C=O}}$ [26] of H_4L^1 , H_4L^2 , H_5L^3 and H_5L^4 ligands are at 1666, 1670, 1681 and 1710 cm^{-1} , respectively, which is shifted in case of $[\text{Fe}(\text{H}_4\text{L}^3)(\text{H}_5\text{L}^3)\text{Cl}_2 \cdot 5\text{H}_2\text{O}]$ and $[\text{Fe}(\text{H}_2\text{L}^4) \cdot 6\text{H}_2\text{O}]$ complexes, suggesting that the carbonyl group is strongly affected on coordination with transition metal ions either by direct interaction between the lone pair of electrons of the carbonyl group with metal ion or through tautomerization. Also, $\delta_{\text{C=O}}$ vibration band reached to the same conclusion. H_4L^2 , H_5L^3 and H_5L^4 compounds gave bands at 1493, 1452 and 1491 cm^{-1} , respectively, identified to azo vibration [27,28]. The shift of this band in all complexes indicated that the azo group is involved in coordination. The presence of $\gamma_{\text{C=O}}$, $\nu_{\text{C=O}}$ [29] modes of vibrations in the metal complexes, suggest that the oxygen atom is also a center of coordination. New bands are appeared in all azo gallic acid complexes in the frequency ranges 437–592 cm^{-1} and 503–646 cm^{-1} , which are attributed to $\nu_{\text{M-N}}$ and $\nu_{\text{M-O}}$, respectively. From the analytical data, electronic spectra and magnetic moment results, Table 4, iron(III)-complexes are of Oh geometry [30,31]. The following chemical equations suggested the formation of the complexes:



DTA of some ligands and their Fe(III) complexes

Differential thermal analysis (DTA) was carried out, where the rate of heating was 10 $^\circ\text{C}/\text{min}$. The order of chemical reactions (n) was calculated via the peak symmetry method [32]. The value of the decomposed substance fraction, (α_m), at the moment of maximum development of reaction with $T = T_m$ being determined from the relation: $(1 - \alpha_m) = n^{1-n}$ [33]. The values of collision factor, Z , can be obtained from the following equation:

$$z = \frac{E}{RT_m} \phi \exp\left(\frac{E}{RT_m^2}\right) = \frac{kT_m}{h} \exp\left(\frac{\Delta S^\ddagger}{R}\right)$$

where ΔS^\ddagger represents the entropy of activation, R molar gas constant, ϕ rate of heating (K s^{-1}), k the Boltzmann constant and h the Planck's constant. The heat of transformation, ΔH^\ddagger , can be calculated from the DTA curves [34]. In general, the change in enthalpy (ΔH^\ddagger) for any phase transformation taking place at any peak

Table 3
Fundamental infrared bands for organic ligands and their iron(III)-complexes.

Compound	ν_{OH}	$\nu_{C=O}$	$\nu_{C=C}$ and ν_{C-C}	$\nu_{N=N}$	ν_{C-OH} and δ_{OH}	δ_{C-OH}	$\delta_{C=O}$ and γ_{CO}	γ_{O-H}	H. bonding OH in COOH	ν_{M-O}	ν_{M-N}
H_4L^1	3494	1666	1612	–	1318	1266	634	865	733	–	–
	3279		1540		1384	1098		794			
	2669		1426								
$Fe(H_4L^1)_3Cl_3 \cdot 4H_2O$	3410	1666	1610	–	1303	1263	655	875	732	471	–
	3341		1538		1383	1097		796			
	2679		1439								
H_4L^2	3452	1670	1595	1493	1306	1244	690	835	750	–	–
	3218		1445		1410	1068					
	3033										
$Fe(H_2L^2)Cl_2 \cdot 2H_2O$	–	–	1579	1510	–	1257	694	840	745	499	603
	3355		–								
	3053										
H_5L^3	3312	1681	1606	1452	1368	1108	663	818	753	–	–
			1518								
			1602								
$Fe(H_4L^3)(H_5L^3)Cl_2 \cdot 5H_2O$	3212	1693	1602	1445	1344	1108	669	833	755	530	607
			1488								
			1601								
H_5L^4	3367	1710	1601	1491	1307	1214	688	879	758	–	–
	3203		1452		1379	1116					
	3072										
$Fe(H_2L^4) \cdot 6H_2O$	3377	1730	1587	1481	1309	1230	684	887	761	445	530
	3188		–		1379	1147					

Table 4
Analytical data, electronic absorption spectra and room temperature magnetic moment values.

Complex	% Calculated/(found)					λ (nm)	μ_{eff}	Electronic transition
	M	C	H	N	X			
$Fe(H_4L^1)_3Cl_3 \cdot 4H_2O$	7.3	33.3	2.9	–	13.9	300,390	5.9	CT ($t_{2g} \rightarrow \pi^*$) CT ($\pi \rightarrow e.g.$)
	(6.8)	(33.7)	(3.5)		(13.5)	450,510		
$Fe(H_2L^2)Cl_2 \cdot 2H_2O$	13.8	39.1	3	7.0	8.7	300,389,675	5.9	CT ($t_{2g} \rightarrow \pi^*$) CT ($\pi \rightarrow e.g.$)
	(13.7)	(39.4)	(3.4)	(7.4)	(8.4)			
$Fe(H_4L^3)(H_5L^3)Cl_2 \cdot 5H_2O$	7.0	39.2	3.6	7	9.0	386,314,350,460,510	5.9	CT ($t_{2g} \rightarrow \pi^*$) CT ($\pi \rightarrow e.g.$)
	(7.2)	(39.8)	(3.7)	(7.3)	(9.5)			
$Fe(H_2L^4) \cdot 6H_2O$	11.6	35.3	3.9	5.8	–	400,485,510,565	5.9	CT ($t_{2g} \rightarrow \pi^*$) CT ($\pi \rightarrow e.g.$)
	(11.0)	(35.8)	(4.4)	(6.1)				

Table 5
DTA ligands and their Fe(III) complexes.

Compound	Type	T_m (°K)	ΔE (kJ/mol ⁻¹)	n	α_m	ΔS^\ddagger (kJ K ⁻¹ mol ⁻¹)	ΔH^\ddagger (kJ mol ⁻¹)	10^3Z (s ⁻¹)
H_4L^1	Endo	379.5	109.1	1.4	0.6	–0.29	–117.2	0.03
	Endo	540.6	439.8	1.2	0.6	–0.29	–156.0	0.09
	Exo	721.8	50.74	0.5	0.7	–0.31	–225.0	0.01
$Fe(H_4L^1)_3Cl_3 \cdot 4H_2O$	Endo	513.5	107.9	1.2	0.6	–0.30	–154.0	0.25
	Exo	623.0	436.6	0.4	0.8	–0.29	–181.0	0.08
	Exo	682.2	468.9	1.6	0.5	–0.29	–199.0	0.08
H_4L^2	Exo	383.0	203.9	1.4	0.6	–0.29	–111.0	0.06
	Exo	833.3	14.37	0.4	0.8	–0.32	–270.0	0.01
	Exo	873.0	143.0	2.3	0.5	–0.31	–267.0	0.02
$Fe(H_2L^2)Cl_2 \cdot 2H_2O$	Exo	373.0	25.73	1.6	0.5	–0.29	–114.0	0.01
	Exo	747.7	484.8	0.7	0.7	–0.27	–219.0	0.07
	Exo	793.0	41.6	1.4	0.6	–0.29	–249.2	0.01
H_5L^3	Exo	373.0	196.0	0.5	0.7	–0.29	–108.0	0.06
	Exo	658.9	4230.0	1.5	0.5	–0.27	–180.0	0.77
	Exo	888.0	1605.0	1.5	0.6	–0.29	–254.0	0.21
$Fe(H_4L^3)(H_5L^3)Cl_2 \cdot 5H_2O$	Exo	903.0	24.71	1.6	0.5	–0.32	–290.0	0.01
	Exo	572.0	196.0	0.7	0.7	–0.29	–169.3	0.04
	Exo	603.0	2006.0	0.5	0.5	–0.27	–167.3	0.40
H_5L^4	Exo	373.0	20.5	0.5	0.5	–0.30	–114.7	0.01
	Exo	705.0	79.2	0.7	0.7	–0.30	–216.4	0.01
	Exo	853.7	383.2	0.7	0.7	–0.29	–253.6	0.05
$Fe(H_2L^4) \cdot 6H_2O$	Endo	588.3	597.2	0.7	0.7	–0.29	–169.0	0.12
	Exo	643.0	10.41	0.6	0.6	–0.32	–207.0	0.01

temperature T_m can be given by the following equation: $\Delta S^\ddagger = \Delta H^\ddagger/T_m$. The (DTA) for H_4L^1 , H_4L^2 , H_5L^3 and H_5L^4 compounds and their Fe(III)-complexes are collected in Table 5. The change of entropy,

ΔS^\ddagger , values for all complexes, are nearly of the same magnitude and lie within the range of (–0.27 to –0.32) kJ K⁻¹ mole⁻¹. So, the transition states are more ordered, the fraction appeared in the

calculated order of the thermal reaction, n , confirmed that the reactions proceeded in the complicated mechanisms. The calculated values of the collision parameters, Z , showed a direct relation to E_a [35]. The values of the decomposed substance fraction (α_m), at maximum development of the reaction were calculated. It is nearly with the same magnitude and lies within the range 0.5–0.8. Based on least square calculations, the $\ln \Delta T$ versus $1000/T$ plots for all complexes gave straight lines from which, the activation energies were calculated [36,37].

Conclusion

Gallic acid and its azo derivatives gave stable complexes with iron(III). These complexes were found to have different metal: ligand ratios. The thermal behavior of these complexes proved that the mechanism of their thermal reactions is not simple where fractions appeared in the calculated orders of these reactions. The calculated values of the collision numbers showed a direct relation to the reactions' activation energies.

Appendix A. Supplementary material

Supplementary data associated with this article can be found, in the online version, at <http://dx.doi.org/10.1016/j.saa.2013.10.054>.

References

- [1] A.S. Li, B. Bandy, S.S. Tsang, *J. Free Rad. Res.* 33 (2000) 551.
- [2] A. Avdeev, S.R. Sofen, T.L. Bregante, K.N. Raymond, *J. Am. Chem. Soc.* 100 (1978) 5362.
- [3] M.J. Hynes, M. O'Coinceannainn, *J. Inorg. Biochem.* 85 (2001) 131.
- [4] H. Kipton, J. Powell, M.C. Talyon, *J. Aust. Chem.* 35 (1982) 739.
- [5] M.S. Masoud, S.S. Hagagg, A.E. Ali, N.M. Nasr, *J. Mol. Struct.* 1014 (2012) 17.
- [6] L.L. Lu, Y.H. Li, X.Y. Lu, *Spectrochim. Acta* 73A (2009) 829.
- [7] T.S. Britton, *Hydrogen Ions*, Chapman. Hall Ltd, London, 1955.
- [8] G. Schwarzenbach, *Complexometric Titration* (H. Irving, Trans), Methuen Co., London, 1957.
- [9] K. Polewski, S. Kniat, D. Slawinska, *Curr. Top Biophys.* 26 (2002) 217.
- [10] I.M. Issa, R.M. Issa, F.I. Taha, M.A. Khattab, *Egypt. J. Chem.* 14 (1971) 59.
- [11] A.A. Muck, M.B. Pravico, *Anal. Chim. Acta* 45 (1969) 534.
- [12] J.C. Colleter, *Z. Ann. Chim.* 5 (1960) 415.
- [13] A.A. Shoukry, M.M. Shoukry, *Spectrochim. Acta* 70A (2008) 686.
- [14] A.E. Harvey, H. Manning, *J. Am. Chem. Soc.* 72 (1950) 4488.
- [15] E. Asmus, *J. Anal. Chem.* 178 (1960) 104.
- [16] A. Holme, F.J. Langmyhr, *Anal. Chim. Acta* 28 (1963) 501.
- [17] P. Jop, *Ann. Chim.* 9 (1928) 113.
- [18] F.W. Fowler, A.R. Katritzky, R.J. Rutherford, *J. Chem. Soc. B* (1971) 460.
- [19] M.S. Masoud, T.M. Salem, M.M. Amer, *J. Rev. Roumaine Chim.* 27 (1982) 235.
- [20] L. Wang, J. Fan, *J. Nano-scale Res. Lett.* 5 (2010) 81.
- [21] F. Billes, I.M. Ziegler, P.J. Bombicz, *Vib. Spectrosc.* 43 (2007) 193.
- [22] I.M. Ziegler, F. Billes, *J. Mol. Struct.* 618 (2002) 259.
- [23] D. Slawins, K. Polewski, P.R. Wski, J.S. Ski, *J. Int. Agrophys.* 21 (2007) 199.
- [24] M.M. Aly, N.I. Al-Shatti, *Trans. Met. Chem.* 23 (1998) 361.
- [25] L.J. Bellamy, *The infrared spectra of complex molecules*, Wiley, New York, 1958.
- [26] A. Kula, *J. Therm. Anal. Calorim.* 75 (2004) 79.
- [27] M.S. Masoud, E.A. Khalil, A.M. Hindawy, A.E. Ali, E.F. Mohamed, *Spectrochim. Acta* 60A (2004) 2807.
- [28] M.S. Masoud, A.E. Ali, R.H. Mohamed, A.A. Mostafa, *Spectrochim. Acta* 62A (2005) 1114.
- [29] D. Hadzi, *J. Chem. Soc.* (1956) 2725.
- [30] D.W. Barnum, *J. Inorg. Nucl. Chem.* 22 (1961) 183.
- [31] N.L. Allinger, J.C. Tai, A.M. Miller, *J. Am. Chem. Soc.* 88 (1966) 4495.
- [32] E. Kissinger, *Anal. Chem.* 29 (1957) 1702.
- [33] M.S. Masoud, T.S. Kasem, M.A. Shaker, A.E. Ali, *J. Therm. Anal. Calorim.* 84 (2006) 549.
- [34] M.L. Dhar, O.J. Singh, *Therm. Anal.* 37 (1991) 259.
- [35] E. Koch, *Thermochim. Acta* 94 (1985) 43.
- [36] M.S. Masoud, A.A. Soayed, A.E. Ali, *Spectrochim. Acta* 60A (2004) 1907.
- [37] R. Iordanova, E. Lefterova, I. Uzunov, Y. Dimitriev, D. Klissurski, *J. Therm. Anal. Calorim.* 70 (2002) 393.